IDENTIFYING FOSSIL KEROGEN IN SEDIMENTARY ROCKS USING RAMAN SPECTROSCOPY.

S. Shkolyar[1], J. D. Farmer[1], and J. Blacksberg[2], [1]School of Earth and Space Exploration, Arizona State University, Tempe, AZ. sshkolya@asu.edu, [2]Jet Propulsion Laboratory, California Institute of Technology, Pasadena, CA.

Introduction: The NRC's 2013-2022 Planetary decadal survey for Solar System Exploration assigned a high priority to Mars sample return (MSR). A Mars sample selection and caching mission, to be launched in 2020, has been identified as the first step in this endeavor. This mission will identify aqueously formed sedimentary rocks at a landing site on Mars, and based upon their enhanced potential for biosignature capture and preservation, will prioritize and cache them for eventual return to Earth. High priority will be given to caching samples that show evidence for past habitable environments and conditions favorable for preservation of fossil biosignatures. One of the most compelling criteria for sample selection will be evidence for fossilized carbonaceous matter (kerogen) of possible biological origin. Such samples will be cached and returned to Earth to look for evidence of fossil biosignatures using more detailed analyses in terrestrial laboratories.

The returned sample volume and mass will likely be restricted to ~30 samples and a total mass of <500 grams [1]. For an effective sample return campaign for Astrobiology, it will be essential that samples selected for the MSR cache will have a high potential for capturing and preserving fossil biosignatures.

Raman spectroscopy is a nondestructive surface technique for analyzing materials *in situ,* with minimal sample preparation. It provides information about both the mineral composition and organic matter present in rock samples.

Study: To better understand the complexities of identifying kerogen in aqueous sedimentary materials using Raman spectroscopy, we surveyed a broad range of sample materials generally regarded to represent high priority habitable environments for the astrobiological exploration of Mars [3]. Lithotypes studied included cherts, carbonates, sulfates, and clay-rich shales. Samples studied covered a range of geological ages and kerogen maturities.

Samples used for the study were also characterized by X-ray Diffraction (XRD) and thin section petrography to provide independent assessments of mineralogy and micropaleontology, and to map the distribution of kerogenous fossil materials present in samples.

Results: The study showed that reliable kerogen identification in most of the lithologies studied is often complicated by high background fluorescence originating from both long (>10 ns to ms) and short (<1 ns) lifetime effects arising from both organic matter as well as the host mineral matrixes.

Some lithotypes, such chert dikes within the Archean Strelley Pool chert, Pilbara region of western Australia, displayed consistently low background fluorescence, enhancing both mineral identifications and kerogen detection (Fig. 1). One possible reason for the lower fluorescence in this sample may be the fluorescence-quenching effects of increased concentrations of poly-aromatic hydrocarbons present in some kerogen types, such as thermally mature kerogen [2] seen in the Strelley Pool chert. Other samples allowed mineral and kerogen identification through high but non-prohibitive fluorescence (Fig. 1).

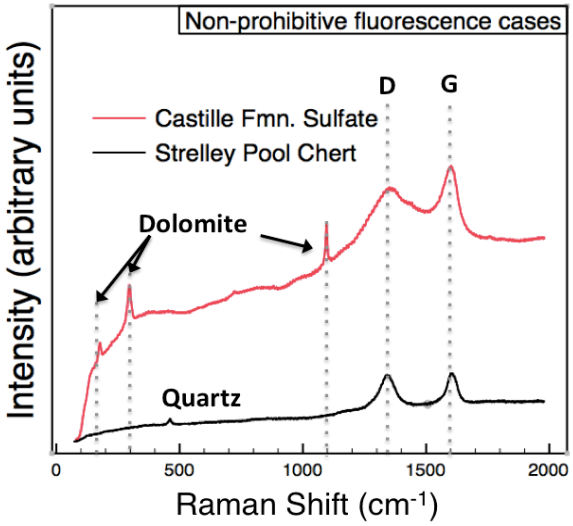

Fig. 1. Non-prohibitive fluorescence in Raman spectra in minerals and kerogen. Raman spectra are shown for kerogen in a carbonate-rich lamination of the Castille Formation sulfate which exhibited high fluorescence but non-prohibitive detection of both 1350 cm^{-1} (D band) and 1600 cm^{-1} (G band) kerogen peaks, as well as dolomite. The chert from Strelley Pool allowed both kerogen bands as well as quartz to be detected. The chert exhibited low fluorescence.

In contrast, carbonate lithotypes (e.g., organic-rich calcareous shale from Green River Formantion, WY) consistently showed high background fluorescence due to contributions from both immature kerogen, and the surrounding carbonate matrix (Fig. 2). In other carbonate examples, such as the stromatolitic limestone sample from Walker Lake, NV, high flurescence prohibited kerogen detection, except at high beam energies, where both matrix minerals and kerogen may have been thermally degraded.

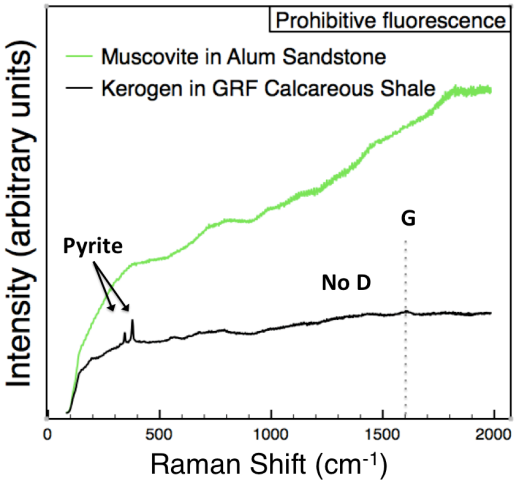

Fig. 2. Prohibitive fluorescence in Raman spectra in minerals and kerogen. In the spectrum of a muscovite grain cemented by carbonate in the Alum sandstone, high fluorescence impeded its detection. Kerogen in an organic-rich lamination between calcite-rich laminations in the Green River Fmn. (GRF) calcareous shale exhibited high fluorescence, allowing only a weak kerogen peak at 1600 cm^{-1} (G band) to be visible, but prohibiting the peak at 1350 cm^{-1} (D band) to be visible due to fluorescence. (Two peaks from pyrite were captured in the sampling volume.)

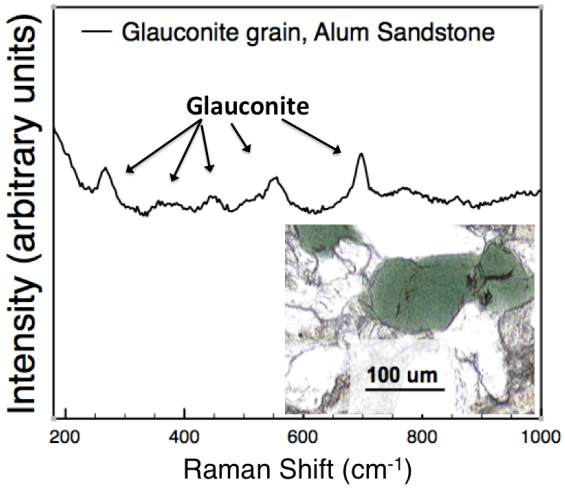

Fig. 3. Potential of time-resolved Raman in identifying minerals through high fluorescence. Glauconite (photomicrograph shown in inset) was detected in the Alum sandstone sample with Time-Resolved Raman spectroscopy. XRD and CW Raman were not successful in definitively identifying it.

It is important to note that both carbonate and chert lithologies are among the most common host rocks for the Precambrian microfossil record on Earth and are-also high-priority targets for in situ analysis and Mars sample return [3].

Work by Blacksberg et al [4, 5] has shown the potential of time-resolved Raman spectroscopy for reducing the effects of high background fluorescence and improving capabilities to detect both kerogen and minerals. In this study, the same time-resolved Raman spectroscopy instrument showed promise in reducing fluorescence where it was prohibitive in some of our Mars analog samples. For example, in the Alum sandstone, glauconite, a phyllosilicate indicative of a marine depositional (habitable) environment, was suspected in microscopy analyses based its color in plane light, birefringence, grain morphology, and friability. It was confirmed as glauconite only with time-resolved Raman (Fig. 3). CW (standard, continuous wave) Raman was unable to confirm its identity due to high fluorescence and XRD did not detect it due to its low abundance. If glauconite were present and detectable by Raman on a Mars lander, along with the 1350 and 1600 cm^{-1} peaks, this represents an ideal example of a sample for caching and return to Earth. It would represent a hydrated phyllosilicate phase indicative of a habitable environment, and one that showed an identification for a carbon biosignature.

Conclusions and Recommendations: Because the sample mass for samples returned to Earth will be limited, effective *in situ* sample selection will be critically important for caching those samples with the highest potential for biosignature preservation at a site. While some lithotypes do not show high background fluorescence, our studies have shown that most of the high priority lithotypes do. If Raman is used to screen for the best samples, it will be important to minimize fluorescence effects in samples to ensure success.

This study recommends: (1) continued research to further evaluate time-resolved Raman techniques to reduce the effects of fluorescence in high-priority target lithologies for Mars and (2) following a science-driven approach to identify and understand the impacts of sample-dependent issues when defining future exploration strategies.

Acknowledgement: Part of the research described here was carried out at the Jet Propulsion Laboratory, California Institute of Technology, under a contract with the National Aeronautics and Space Administration (NASA). Erik Alerstam and Yuki Maruyama of JPL are acknowledged for assistance with data collection on the time-resolved Raman.

References: [1] Mars 2020 SDT (2013), Committee members: Mustard, J. F. (chair), et al.: Report of the Mars 2020 Science Definition Team, 154 pp., http://mepag.jpl.nasa.gov/reports/MEP/Mars_2020_SDT_Report_Final.pdf. [2] Bertrand, P. et al. (1985) *Advances in Organic Geochemistry*, *10*, 641-7. [3] Farmer, J. D. & Des Marais, D. J. (1999) *JGR 104*, 26977. [4] Blacksberg, J. et al. (2014) *45th LPSC*, Abstract #1544. [5] Blacksberg, J. et al. (2013) *2013 AGU*, Abstract # P51G-1803.